Near complete local reduction of Arctic stratospheric ozone by severe chemical loss in spring 2020

I. Wohltmann[1], P. von der Gathen[1], R. Lehmann[1], M. Maturilli[1], H. Deckelmann[1], G. L. Manney[2,3], J. Davies[4], D. Tarasick[4], N. Jepsen[5], R. Kivi[6], N. Lyall[7]and M. Rex[1]

[1]Alfred Wegener Institute for Polar and Marine Research, Potsdam, Germany
[2]NorthWest Research Associates, Socorro, New Mexico, United States
[3]New Mexico Institute of Mining and Technology, Socorro, New Mexico, United States
[4]Air Quality Research Division, Environment and Climate Change Canada, Downsview, ON, Canada
[5]Danish Meteorological Institute, Copenhagen, Denmark
[6]Finnish Meteorological Institute, Space and Earth Observation Centre, Sodankylä, Finland
[7]UK Met Office, Lerwick Observatory, Shetland Islands, UK

Key Points:

- Local minimum ozone mixing ratios of 0.1–0.2 ppm observed by sondes in Arctic spring 2020 are significantly lower than in any previous year.
- Local ozone loss (93 %) and mixing ratios are comparable to typical values in the Antarctic ozone hole (95 %–99 %, 0.01–0.1 ppm).
- The reason for the unprecedented chemical loss was an unusually strong, long-lasting, and record cold polar vortex.

Corresponding author: Ingo Wohltmann, ingo.wohltmann@awi.de

Abstract

In the Antarctic ozone hole, ozone mixing ratios have been decreasing to extremely low values of 0.01–0.1 ppm in nearly all spring seasons since the late 1980s, corresponding to 95–99 % local chemical loss. In contrast, Arctic ozone loss has been much more limited and mixing ratios have never before fallen below 0.5 ppm. In Arctic spring 2020, however, ozone sonde measurements in the most depleted parts of the polar vortex show a highly depleted layer, with ozone loss averaged over sondes peaking at 93 % at 18 km. Typical minimum mixing ratios of 0.2 ppm were observed, with individual profiles showing values as low as 0.13 ppm (96 % loss). The reason for the unprecedented chemical loss was an unusually strong, long-lasting and cold polar vortex, showing that for individual winters the effect of the slow decline of ozone-depleting substances on ozone depletion may be counteracted by low temperatures.

Plain Language Summary

The severe chemical ozone loss in the Antarctic ozone hole and its impact on human health and climate have generated widespread public, political, and scientific interest. In contrast, Arctic ozone reduction has been much more limited because of higher temperatures and more variability in transport in the northern hemisphere (lower temperatures lead to more chemical loss and more transport can increase ozone values). In Arctic spring 2020, however, observations of balloon sondes and satellites show that locally, absolute values of ozone (measured in mixing ratios, i.e., molecules of ozone per molecules of air) are significantly lower than in any previous year and are comparable to typical local values in the Antarctic ozone hole, albeit over a much narrower layer. Locally, the chemical loss of ozone peaked at 93 % in Arctic spring 2020, compared to values of 95 %–99 % in the Antarctic. The reason for the unprecedented loss was unusually cold and stable conditions in the Arctic stratosphere.

1 Introduction

The discovery of the Antarctic ozone hole in the 1980s (Farman et al., 1985) and of its impact on human health and climate generated widespread public, political, and scientific interest (e.g. WMO, 2018). Soon, chlorine and bromine released from decomposition of man-made chlorofluorocarbons (CFCs) and other ozone-depleting substances (ODS) in the upper atmosphere were identified as the cause of the ozone hole (Solomon et al., 1986). Chlorine is transformed from inactive reservoir gases to active chlorine species at the surfaces of polar stratospheric clouds, which only form at very low temperatures in polar winter. With the return of sunlight in spring, ozone is depleted by photochemical catalytic cycles. As a consequence of these discoveries, the production of CFCs was phased out by the Montreal protocol and chlorine levels have been slowly declining in recent years (e.g. WMO, 2018).

Ozone volume mixing ratios have been decreasing to extremely low values of 0.01–0.1 ppm in nearly all Antarctic spring seasons since the late 1980s in a wide altitude range from 360–510 K potential temperature (12–20 km) (e.g. Solomon et al., 2014; Kuttippurath et al., 2018), corresponding to about 95 %–99 % local chemical ozone loss. In recent decades, Antarctic ozone loss has reached saturation and is not expected to get any more severe (e.g. Kuttippurath et al., 2018). Early signs of a recovery due to the success of the Montreal protocol have been reported (e.g. Kuttippurath et al., 2018; WMO, 2018).

In contrast to the Antarctic, ozone depletion in the Arctic is usually much less pronounced and shows a much higher interannual variability because of the significantly higher stratospheric temperatures and higher dynamical activity in the Northern hemisphere (e.g. Solomon, 1999; Tegtmeier et al., 2008; Manney et al., 2011; Solomon et al., 2014).

In addition to less pronounced depletion, ozone loss is masked by the variability of ozone transport in the northern hemisphere. On average, the variability of chemistry and transport contribute about equally to the interannual variability in polar ozone (Tegtmeier et al., 2008).

Ozone loss in the Arctic has ranged from almost no ozone loss in warm winters (e.g. 1998/1999, 2018/2019) to the most severe depletion observed so far in the winter 2010/2011. Values reported for the ozone loss in 2010/2011 range from 2.3–2.6 ppm for the maximum loss in the vortex mean profile, corresponding to 60–80 % relative loss, and 84–120 DU for the column loss (e.g. Manney et al., 2011; Sinnhuber et al., 2011; Kuttippurath et al., 2012; Strahan et al., 2013; Pommereau et al., 2013; Hommel et al., 2014; Solomon et al., 2014). The wide range of values highlights the inherent uncertainty in calculating ozone loss caused by using different methods, data sets, vortex edge definitions, or altitude ranges (Livesey et al., 2015; Griffin et al., 2019). Local minimum volume mixing ratios of about 0.5 ppm were observed in the winter 2010/2011 (Manney et al., 2011; Hommel et al., 2014; Solomon et al., 2014). Several authors noted that the ozone loss in 2011 might arguably be called an Arctic ozone hole (e.g., Manney et al., 2011; Sinnhuber et al., 2011), although this is highly controversial (e.g., Solomon et al., 2014). Here, we show that local ozone reduction in the winter 2019/2020 considerably exceeded the values reached in 2010/2011 and that extremely low absolute values of ozone of 0.1–0.2 ppm were reached in some parts of the vortex for the first time.

The reason for the unprecedented loss was an unusually strong, long-lasting and record cold polar vortex (see Lawrence et al., this issue, e.g. Fig. 10, 11). The vortex lasted until early to mid May and showed temperatures below the formation temperature of polar stratospheric clouds from mid November to late March through early April (depending on altitude). The only winters previously observed in which low temperatures lasted until the end of March were 1996/1997 and 2010/2011 (Manney et al., 2011), and only the winters 1996/1997, 2004/2005, and 2010/2011 showed periods below the formation temperature of polar stratospheric clouds of length comparable to 2019/2020 so far (e.g., Manney et al., 2011), while the total volume of air exposed to low temperatures was larger in 2019/2020 than in any previous winter.

This is consistent with a tendency of the coldest Arctic winters to become colder in recent decades, which has been suggested by several studies (Rex et al., 2004, 2006; Tilmes et al., 2006; Sinnhuber et al., 2011; von der Gathen et al., 2020). This suggestion has been controversial, with other studies using different metrics, meteorological data sets (Lawrence et al., 2018), or statistical methods finding the trend to be limited to certain months (Ivy et al., 2014) or not significant (Manney et al., 2011; Rieder & Polvani, 2013). Nevertheless this tendency is found for the temperature metric used in this study. A tendency for Arctic winters to become colder in turn is expected to lead to increasing ozone loss in these winters (Rex et al., 2004, 2006; Tilmes et al., 2006; Harris et al., 2010; von der Gathen et al., 2020).

Large interannual variability in temperatures and the occurrence of cold winters are expected to extend into the future (Langematz et al., 2014; Bednarz et al., 2016; von der Gathen et al., 2020). While the slow decline in ozone-depleting substances will lead to a complete recovery of the ozone layer in a few decades, this large variability can counteract those effects in individual winters (Eyring et al., 2010; Dhomse et al., 2018; WMO, 2018). There is however considerable uncertainty in the future trend of Arctic stratospheric temperatures in both cold and more dynamically active warm winters (Butchart et al., 2010; Eyring et al., 2010; Langematz et al., 2014). These changes are determined by a complex interplay of increases in radiative cooling induced by the growth in greenhouse gases and by dynamical changes, such as changes in the strength of the adiabatic warming induced by changes in the polar downwelling of the Brewer-Dobson circulation (Butchart et al., 2010; Eyring et al., 2010; Langematz et al., 2014).

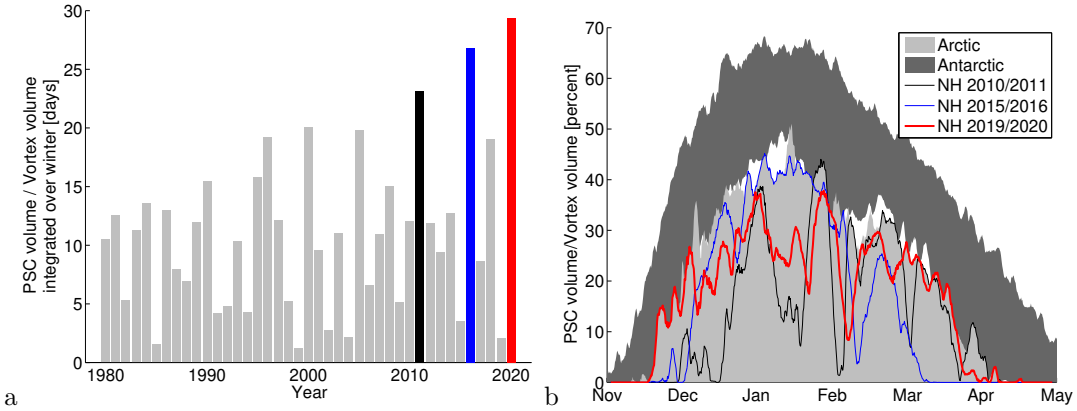

Figure 1. **a** Fraction of Arctic polar vortex volume below the formation temperature of polar stratospheric clouds ($V_{\mathrm{PSC}}/V_{\mathrm{vortex}}$) integrated over the winter (November–April) for different years. The 3 coldest winters by this metric are marked in black (2010/2011), blue (2015/2016) and red (2019/2020). **b** Fraction of polar vortex volume below the formation temperature of polar stratospheric clouds as a function of season. The red line shows Arctic values for 2019/2020, the thin lines show values for the years 2010/2011 (black) and 2015/2016 (blue), using the same colors as Figure 1. Light and dark shading shows range of Arctic and Antarctic values for 1979–2020. Antarctic values are shifted by half a year.

2 Results

2.1 Temperatures

A particularly useful measure of the temperatures in the polar vortex is the volume V_{PSC} of air below the threshold temperature for the formation of polar stratospheric clouds composed of nitric acid trihydrate (e.g. Rex et al., 2004, 2006; Tilmes et al., 2006; Harris et al., 2010; Manney et al., 2011). This threshold temperature is also comparable to the temperature below which chemical processing of chlorine reservoir gases on the other important cloud type (supercooled ternary $H_2SO_4/HNO_3/H_2O$ solutions) becomes important (e.g., Spang et al., 2018). It has been shown empirically that there is a high correlation between V_{PSC} integrated over the Arctic winter and the overall ozone loss integrated over the winter (e.g. Rex et al., 2004, 2006; Tilmes et al., 2006; Harris et al., 2010; Pommereau et al., 2018), and attempts have been made to explain this correlation (Harris et al., 2010). A related quantity refining the concept of V_{PSC} is the quantity $V_{\mathrm{PSC}}/V_{\mathrm{vortex}}$, which takes into account the volume of the vortex V_{vortex} (e.g., Tilmes et al., 2006, 2008; Manney et al., 2011; von der Gathen et al., 2020) and is expected to correlate better with vortex averaged ozone loss and also to be more directly comparable between the Arctic and the Antarctic.

The stratospheric winter 2019/2020 was the coldest winter on record in the last 41 years in terms of $V_{\mathrm{PSC}}/V_{\mathrm{vortex}}$ integrated over the winter. Figure 1 **a** shows the time series of Arctic $V_{\mathrm{PSC}}/V_{\mathrm{vortex}}$ integrated over November–April for 1979/1980–2019/2020 based on meteorological data from the European Centre for Medium-range Weather Forecasts (ECMWF) ERA5 reanalysis with 0.28125° horizontal resolution and 6 h temporal resolution (Hersbach et al., 2020). See Lawrence et al., this issue, for similar calculations for the MERRA reanalysis.

Here and in the following, the vortex edge was assumed at 36 PVU potential vorticity at 475 K and the definition was extended to other altitudes by the method used in Rex et al. (1999). The fraction of the vortex volume below the formation tempera-

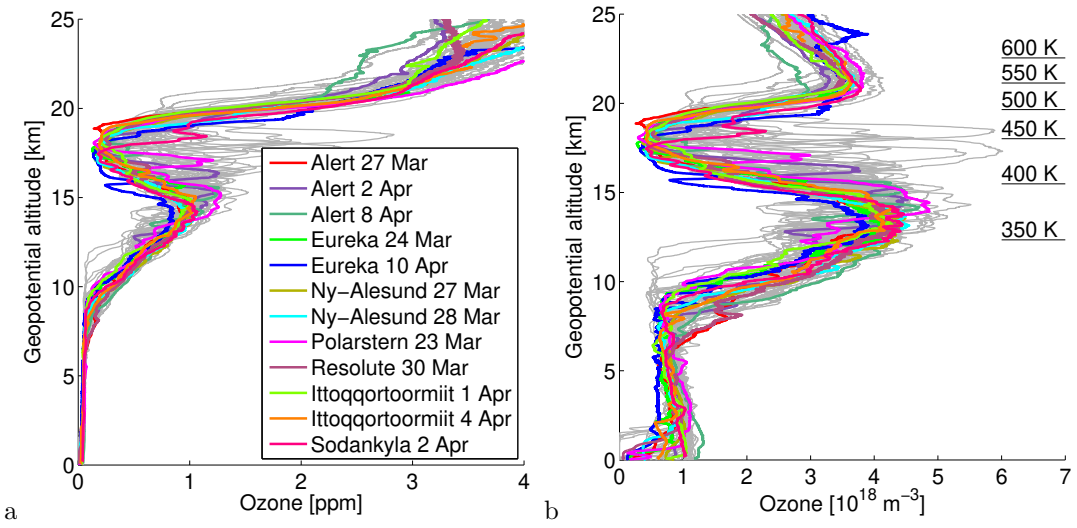

Figure 2. Ozone sonde profiles inside the polar vortex from 23 March to 10 April 2020 as a function of altitude (**a** volume mixing ratios, **b** ozone number concentrations). A set of 12 sondes was chosen from all measurements to represent the air masses most depleted in ozone (colored lines). All other profiles are shown in grey. Approximate potential temperature levels corresponding to the altitudes are indicated.

ture of polar stratospheric clouds composed of nitric acid trihydrate was calculated as in Hanson and Mauersberger (1988). A volume mixing ratio of 4.6 ppm was assumed for H_2O. The mixing ratio profile of HNO_3, which varies as a function of pressure, is based on measurements acquired in the Arctic during January 1979 by the Limb Infrared Monitor of the Stratosphere (LIMS) on board Nimbus 7 (Remsberg et al., 2010). The altitude range for the vertical integration is 400–700 K. For Figure 1 **a**, instantaneous values of $V_{\mathrm{PSC}}/V_{\mathrm{vortex}}$ (dimensionless) were integrated from November to April, yielding a value in units of time.

It appears that the coldest Arctic winters have become colder in recent decades. The record for the coldest winter has been broken typically every 5 years and an increase by a factor of 3 of the $V_{\mathrm{PSC}}/V_{\mathrm{vortex}}$ metric from 1979/1980 to 2019/2020 is observed in these winters (von der Gathen et al., 2020).

The three coldest Arctic stratospheric winters on record by integrated $V_{\mathrm{PSC}}/V_{\mathrm{vortex}}$ all occurred in the last 10 years: 2010/2011, 2015/2016 and 2019/2020. Figure 1 **b** shows the seasonal evolution of these three winters in terms of daily values of $V_{\mathrm{PSC}}/V_{\mathrm{vortex}}$, compared to the range of Arctic and Antarctic values. The former record holder for the coldest winter (2010/2011) showed the largest Arctic ozone loss so far (e.g. Manney et al., 2011; Sinnhuber et al., 2011; Hommel et al., 2014). The winter 2015/2016 showed greater values of V_{PSC} (and lower temperatures) until February, but less ozone loss due to an early warming of the polar vortex (Manney & Lawrence, 2016; Khosrawi et al., 2017). While low temperatures at the end of March lasted for a few days longer in the winter 2010/2011 than in 2019/2020, this was offset by lower temperatures in 2019/2020 than in 2010/2011 in early winter (December and January). In early winter, 2015/2016 and 2019/2020 had similar temperatures.

2.2 Ozone

Figure 2 shows all 52 ozone sonde profiles measured inside the polar vortex from 23 March to 10 April 2020 (grey and colored lines). We selected a set of 12 ozone sonde measurements from this time period to represent the air masses most depleted in ozone inside the polar vortex (colored lines). This set is intended to exemplify the maximum ozone loss in spring 2020. As a selection criterion, we chose all profiles with a minimum mixing ratio less than 0.2 ppm anywhere in an altitude range of 370–550 K. These sonde measurements were performed in Alert (82.5° N, 62.3° W; 27 March, 2 April, 8 April), Eureka (80.0° N, 85.9° W; 24 March, 10 April), Ny-Ålesund (78.9° N, 11.9° E; 27 March, 28 March), Ittoqqortoormiit (Scoresbysund) (70.5° N, 22.0° W; 1 April, 4 April), Resolute (74.7° N, 94.9° W; 30 March) and Sodankylä (67.4° N, 26.6° E; 2 April). One of the profiles was measured onboard Polarstern in the Arctic Ocean (86.2° N, 15.8° E; 23 March) during the MOSAiC expedition.

In addition, we use satellite observations of ozone mixing ratio from the Microwave Limb Sounder (MLS) instrument to confirm the findings from the sondes. While sonde measurements have a higher vertical resolution and higher accuracy and precision than the MLS instrument, the temporal and spatial measurement coverage of the vortex is much better for MLS: There are several hundred profile measurements in the vortex from MLS every day, but typically only 5–10 ozone soundings per week. The estimated precision and accuracy of the MLS instrument in the considered altitude range are 0.04–0.06 ppm and 0.1–0.2 ppm (Livesey et al., 2020), which are in the same order of magnitude as the lowest values measured by the sondes in spring 2020. The precision of the ozone sondes is ±(3–5)% and the accuracy ±(5–10)% (Smit et al., 2007).

A simple estimate of the fraction of the vortex area subject to the largest depletion, found by taking the 12 soundings of 52 to be representative, is 23 %. The corresponding estimate calculated from MLS observations inside the vortex that were below 0.2 ppm at 450 K is 12 %, averaged between 26 March and 10 April.

All sonde profiles consistently show a pronounced depleted layer in ozone concentrations and mixing ratios between 425 K and 485 K (17–19 km). The lowest values are observed around 450 K (18 km). Most profiles show minimum volume mixing ratios of about 0.15–0.2 ppm. The lowest mixing ratio in an individual sonde (0.13 ppm) was observed in a profile measured in Eureka on 24 March. The minimum values are observed near the altitudes that typically show the maximum ozone number concentrations in warm winters with low ozone depletion (about 400 K).

The observed minimum values are by far lower than any minimum values observed by sondes or the MLS instrument in the Arctic polar vortex before, which did not fall below 0.5 ppm even in 2010/2011 (e.g., Solomon et al., 2014). Figure 3 **a**, **b** show the daily minimum mixing ratios observed by sondes in the altitude range 420–480 K in the Arctic polar vortex in 1991/1992–2010/2011, 2015/2016 and 2019/2020 and in the Antarctic polar vortex in 1985–2019 (in linear and logarithmic scale). Antarctic data are from two stations: Georg Forster (70.8° S, 11.9° E) and Neumayer (70.7° S, 8.3° W). The altitude range has been chosen since it always contains the ozone minimum in the cold Arctic winters 2010/2011 and 2019/2020. The Arctic winters 2010/2011 (black), 2015/2016 (blue) and 2019/2020 (red) are highlighted.

The strong decline of the values in 2019/2020 to minimum values around 0.2 ppm is remarkably similar to the typical evolution of the values in Antarctic winters (dark grey), although smaller values of up to 0.01 ppm are commonly reached in the Antarctic. Minimum values in the Arctic in 2010/2011 (0.5 ppm) and 2015/2016 (1.25 ppm) were significantly higher. To corroborate the results from the sondes, Figure 3 **c**, **d** show the daily mean mixing ratios of the lowest 10 % of measurements observed in the polar vortex by MLS at 56 hPa or 68 hPa in the winters 2004/2005 to 2019/2020 (see also com-

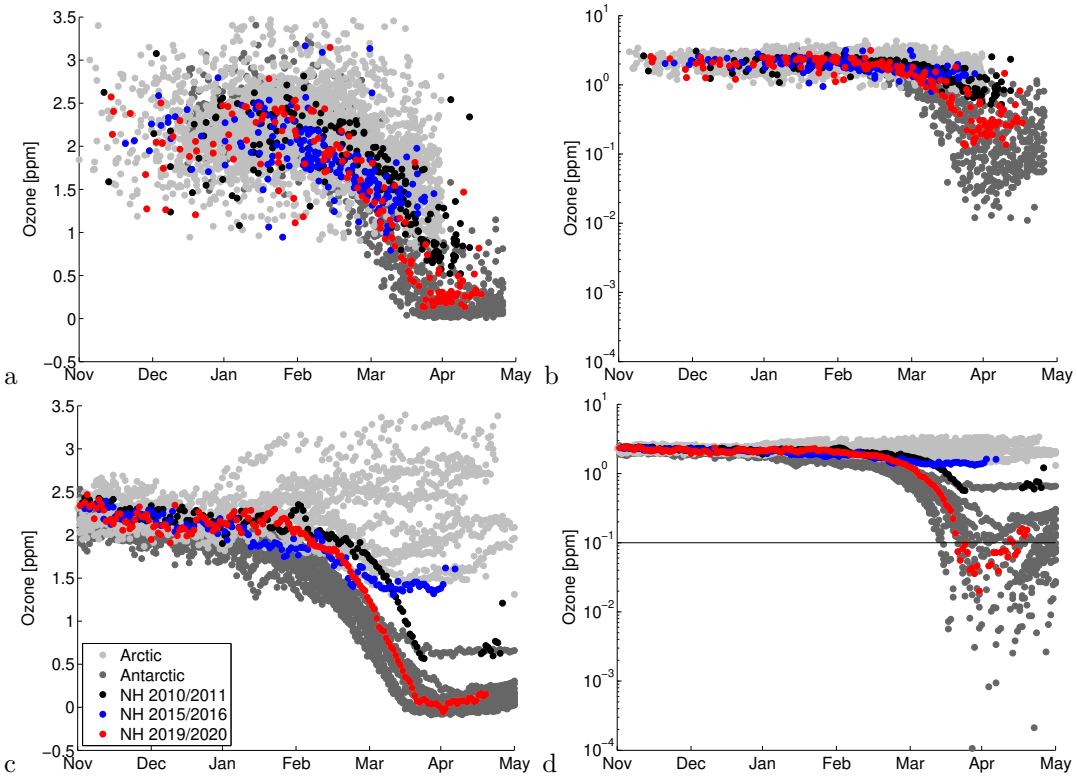

Figure 3. **a** Daily minimum ozone mixing ratios observed by sondes in the polar vortex in the altitude range 420–480 K. The Arctic winters 2010/2011, 2015/2016 and 2019/2020 are highlighted using the same colors as Figure 1. The light and dark grey points show the range of Arctic values (1991/1992–2010/2011) and Antarctic values (1985–2019). Antarctic values are shifted by half a year. **b** Same plot in logarithmic coordinates. **c** Daily mean mixing ratios of the lowest 10 % of measurements of the MLS satellite instrument in the polar vortex at 56 hPa or 68 hPa for the winters 2004/2005–2019/2020, shown in the same manner as in **a**. The lowest 10 % of measurements are used instead of the daily minimum to reduce the influence of measurement noise on the measured minima. **d** Same plot in logarithmic coordinates. The line shows the approximate combined precision and accuracy of the MLS measurements.

plementary figures S1–S3 in Manney et al., this issue, for map and profile views). The MLS retrieval levels 56 hPa and 68 hPa have been chosen since they always contain the measured minimum values in the cold winters 2010/2011 and 2019/2020. Differences between Figure 3 **a** and **c** can be explained by the different vertical resolutions of the instruments, different coverage of the vortex, and the use of minimum values versus averages over the lowest 10 % of measurements.

Values measured by MLS even fall to near zero or below due to measurement noise. The lowest 10 % of measurements are used instead of a single daily minimum value to reduce the influence of measurement noise on the minima, since the noise is in the same order of magnitude as the lowest values of 0.2 ppm measured by sondes. Taking observed minimum values will always underestimate the true minima of a noisy measurement, but the degree of underestimation will be dependent on the measurement noise and the unknown distribution of the true measurement values. Hence, we cannot deduce the measured minimum from MLS with certainty, but it seems likely that the measurements are consistent with the lowest values of 0.2 ppm observed by the sondes.

2.3 Ozone loss

Figure 4 **a**, **c**, **e** show the ozone loss observed by sondes in the most depleted part of the vortex as a function of altitude, averaged over all 12 profiles. Ozone loss is calculated as the difference between a passive ozone tracer from the global Lagrangian ATLAS Chemistry and Transport Model (Wohltmann & Rex, 2009) and the observed sonde profile. Transport and mixing in the model were driven by winds and temperatures from ECMWF ERA5 meteorological reanalysis data (1.125° horizontal resolution, 3 h temporal resolution). The model uses a hybrid vertical coordinate, which is to a good approximation a potential temperature coordinate in the stratosphere. Diabatic heating rates from ERA5 were used to calculate vertical motion. The vertical range of the model domain is 350–1900 K. The passive ozone tracer was initialized on 1 December 2019 with ozone observations of MLS. The satellite measurements were interpolated to the location of the model air parcels and the air parcels were then advected with ozone as a conserved tracer with the ozone chemistry of the model switched off. The passive ozone tracer is then interpolated to the location of each of the sondes.

Reliable values for the ozone loss can be deduced with this method only from 370–550 K for several reasons: (1) For air masses that entered the model domain after 1 December through the lower or upper boundary, neither the initial position nor the mixing ratio on 1 December are known. A passive potential temperature tracer indicates that values of the passive ozone tracer above 550 K are not reliable because of descent in the polar vortex. At the lower boundary, we excluded all values in the lowermost stratosphere below 370 K, where horizontal transport between the troposphere and stratosphere is possible along isentropes; (2) Above 550 K, NO_x chemistry becomes important; (3) With increasing altitude, ozone becomes more short-lived and approaches equilibrium, which is not compatible with the idea of a passive ozone tracer.

The shape of the loss profile resembles the shape of the minimum of the ozone sonde profiles, and shows values of enhanced ozone loss in a layer from 425–485 K with a maximum loss at 450 K. The minimum in ozone concentrations and mixing ratios at 450 K corresponds to a maximum chemical loss of about 2.8 ppm or 93 %, averaged over all sondes. The maximum loss in an individual profile is 96 %. The partial ozone column averaged over the sondes between 370–550 K is 59±11 DU, and the ozone loss in the partial column is 124 ± 11 DU.

The ozone loss in the most depleted parts of the vortex has to be clearly distinguished from the polar vortex mean loss, which is necessarily less pronounced. Figure 4 **b**, **d**, **f** show the vortex averaged ozone loss for the winters 2010/2011 and 2019/2020 obtained by subtracting MLS measurements of ozone from the passive ozone tracer of the ATLAS

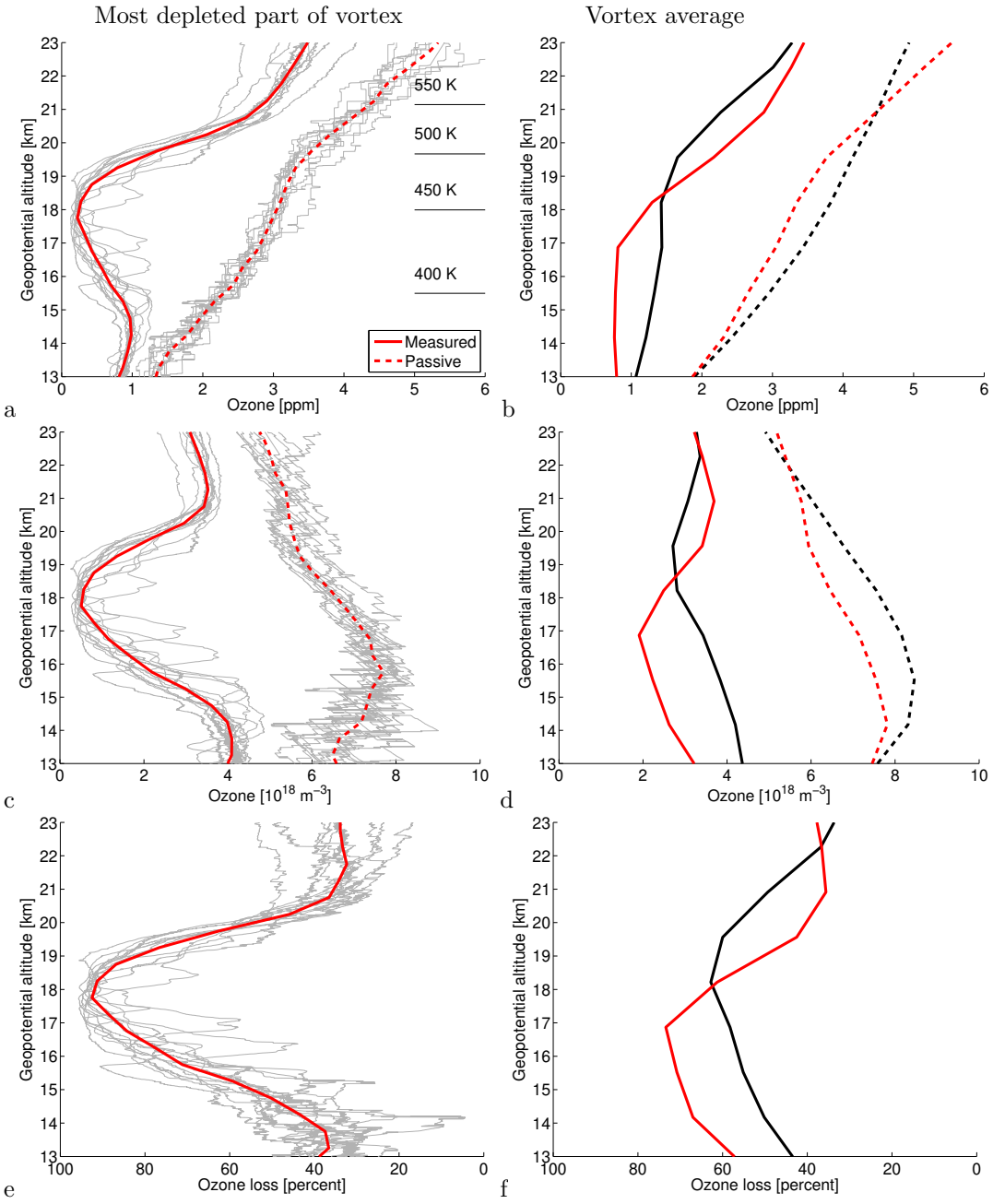

Figure 4. Measured ozone volume mixing ratio (**a**, **b**), corresponding ozone number concentrations (**c**, **d**) and ozone loss in percent (**e**, **f**) calculated by using a passive tracer from the Chemistry and Transport Model ATLAS. **a**, **c**, **e** show averages over the 12 selected ozone sondes in the most depleted part of the vortex. **b**, **d**, **f** show vortex averages calculated using MLS satellite data. The dashed lines in **a**, **b**, **c**, **d** show the passive ozone tracer from ATLAS used to calculate the ozone loss in **e**, **f**. Red lines show averages for 2019/2020, black lines averages for 2010/2011 and grey lines show individual measurements or passive tracer values, respectively.

model in the altitude range 370–550 K inside the polar vortex. The passive ozone tracer was initialized on 1 December again.

The maximum ozone loss in the vortex mean profile in 2019/2020 was about 2.2 ppm at 450 K shortly before the breakup of the vortex (17 April 2020). The corresponding maximum loss for 2010/2011 was 2.5 ppm at 490 K (26 March 2011). The passive profile shows larger values in 2011, so that a reason for the larger loss could be that more ozone was available for depletion. The percentage of loss was generally higher in 2019/2020 and peaks at 73 % at 450 K, compared to a value of 63 % at 470 K in 2010/2011. The winter 2019/2020 shows considerably lower vortex mean mixing ratios than the winter 2010/2011 below 475 K (e.g. 0.8 ppm vs. 1.4 ppm at 450 K), and ozone loss peaked at lower altitudes in 2019/2020 than in 2010/2011. This explains the higher percentage loss but lower absolute loss. Within the uncertainties in empirical ozone loss estimates, these results are consistent with those of Manney et al. (this issue) using different methods. The vortex averaged column loss between 370–550 K was 133 DU in 2010/2011 and 126 DU in 2019/2020.

Taking into account the uncertainties in calculating ozone loss, the vortex mean loss in the winters 2010/2011 and 2019/2020 is rather similar, notwithstanding some morphological differences. To highlight the sources of the uncertainties, we note here that using different meteorological data sets (ECMWF operational data, ERA5 and ERA Interim) will vary the loss estimates in 2010/2011 between 2.2 and 2.5 ppm.

3 Discussion

The minimum ozone mixing ratios of 0.1–0.2 ppm observed in Arctic spring 2020 are significantly lower than observed in any previous year (with lowest values of 0.5 ppm in 2011) and are comparable to typical mixing ratios in the Antarctic ozone hole. In the vortex averaged total column, Arctic chemical loss was similar in 2010/2011 and 2019/2020. One of the reasons for the observed low mixing ratios in 2020 may have been that the dynamical supply of ozone was smaller in the winter 2019/2020, as indicated by the lower values of the passive ozone tracer compared to 2010/2011 and consistent with a weaker residual circulation in cold winters (e.g., Tegtmeier et al., 2008). A weaker residual circulation means less downwelling and less transport of ozone-rich air from above. Interestingly, MLS measurements show lower N_2O and higher H_2O mixing ratios compared to other winters (Manney et al., this issue), which at first glance could also be caused by *more* downwelling; however, evidence in this case suggests it is caused primarily by descent of N_2O values that already were anomalously low in fall (and anomalously high in case of H_2O) and a more isolated vortex (Manney et al., this issue).

While it is estimated that stratospheric ozone levels will eventually return to pre-1980 conditions around 2035 in the Arctic and 2060 in the Antarctic (Dhomse et al., 2018; WMO, 2018), because of the decline in ozone-depleting substances, it is expected that even around 2060, cold winters could still lead to substantial ozone depletion and show values as much as 100 DU lower than the future average (Bednarz et al., 2016). The winter 2019/2020 is a prime example of such a winter. For the first time, almost complete ozone depletion was observed in a limited region and altitude range in the Arctic vortex and the vortex averaged loss was among the largest ever observed in the Arctic, although stratospheric levels of ODS have started to decline since the year 2000.

Acknowledgments
We are grateful to the operating staff of all participating stations for having made the ozone sonde campaign in 2019/2020 possible. Some ozonesonde data used in this manuscript data used in this manuscript were produced as part of the international Multidisciplinary drifting Observatory for the Study of the Arctic Climate (MOSAiC) with the tag MO-

SAiC20192020 (project id AWI_PS122_00). We thank ECMWF for providing ERA5 reanalysis data, generated using Copernicus Climate Change Service Information 2020. Neither the European Commission nor ECMWF is responsible for any use that may be made of the Copernicus Information or Data it contains. Copernicus Climate Change Service (C3S) (2017): ERA5: Fifth generation of ECMWF atmospheric reanalyses of the global climate. Copernicus Climate Change Service Climate Data Store (CDS), 2017–2020.

Ozone sonde data are available on request from the authors and will be available from the World Ozone and Ultraviolet Radiation Data Centre (WOUDC) at https://woudc.org and the Network for the Detection of Atmospheric Composition Change (NDACC) at https://www.ndacc.org. MLS data are available at https://disc.gsfc.nasa.gov/datasets?page=1&keywords=AURA%20MLS. ECMWF ERA5 data are available at https://cds.climate.copernicus.eu/cdsapp#!/home. ATLAS model runs are available upon request from the authors.

References

Bednarz, E. M., Maycock, A. C., Abraham, N. L., Braesicke, P., Dessens, O., & Pyle, J. A. (2016). Future Arctic ozone recovery: the importance of chemistry and dynamics. *Atmos. Chem. Phys.*, *16*, 12159–12176. doi: 10.5194/acp-16-12159-2016

Butchart, N., Cionni, I., Eyring, V., Shepherd, T. G., Waugh, D. W., Akiyoshi, H., ... Tian, W. (2010). Chemistry–climate model simulations of twenty-first century stratospheric climate and circulation changes. *J. Clim.*, *23*, 5349–5374. doi: 10.1175/2010JCLI3404.1

Dhomse, S., Kinnison, D., Chipperfield, M., Cionni, I., Hegglin, M., Abraham, N. L., ... Zeng, G. (2018). Estimates of ozone return dates from Chemistry-Climate Model Initiative simulations. *Atmos. Chem. Phys.*, *18*, 8409–8438. doi: 10.5194/acp-18-5408-218

Eyring, V., Cionni, I., Bodeker, G. E., Charlton-Perez, A. J., Kinnison, D. E., Scinocca, J. F., ... Yamashita, Y. (2010). Multi-model assessment of stratospheric ozone return dates and ozone recovery in CCMVal-2 models. *Atmos. Chem. Phys.*, *10*, 9451–9472.

Farman, J. C., Gardiner, B. G., & Shanklin, J. D. (1985). Large losses of total ozone in Antarctica reveal seasonal ClOx/NOx interaction. *Nature*, *315*, 207-210.

Griffin, D., Walker, K. A., Wohltmann, I., Dhomse, S. S., Rex, M., Chipperfield, M. P., ... Tarasick, D. (2019). Stratospheric ozone loss in the Arctic winters between 2005 and 2013 derived with ACE-FTS measurements. *Atmos. Chem. Phys.*, *19*, 577–601. doi: 10.5194/acp-19-577-2019

Hanson, D., & Mauersberger, K. (1988). Laboratory studies of the nitric acid trihydrate: Implications for the south polar stratosphere. *Geophys. Res. Lett.*, *15*(8), 855-858.

Harris, N. R. P., Lehmann, R., Rex, M., & von der Gathen, P. (2010). A closer look at Arctic ozone loss and polar stratospheric clouds. *Atmos. Chem. Phys.*, *10*, 8499-8510.

Hersbach, H., Bell, B., Berrisford, P., Hirahara, S., Horányi, A., Muñoz-Sabater, J., ... Thépaut, J.-N. (2020). The ERA5 global reanalysis. *Quarterly Journal of the Royal Meteorological Society*. doi: 10.1002/qj.3803

Hommel, R., Eichmann, K.-U., Aschmann, J., Bramstedt, K., Weber, M., von Savigny, C., ... Burrows, J. P. (2014). Chemical ozone loss and ozone mini-hole event during the Arctic winter 2010/2011 as observed by SCIAMACHY and GOME-2. *Atmos. Chem. Phys.*, *14*(7), 3247–3276. doi: 10.5194/acp-14-3247-2014

Ivy, D. J., Solomon, S., & Thompson, D. W. J. (2014). On the identification of the downward propagation of Arctic stratospheric climate change over recent

decades. *J. Climate*, *27*, 2789–2799. doi: 10.1175/jcli-d-13-00445.1

Khosrawi, F., Kirner, O., Sinnhuber, B.-M., Johansson, S., Höpfner, M., Santee, M. L., ... Braesicke, P. (2017). Denitrification, dehydration and ozone loss during the 2015/2016 Arctic winter. *Atmos. Chem. Phys.*, *17*(21), 12893–12910. doi: 10.5194/acp-17-12893-2017

Kuttippurath, J., Godin-Beekmann, S., Lefèvre, F., Nikulin, G., Santee, M. L., & Froidevaux, L. (2012). Record-breaking ozone loss in the Arctic winter 2010/2011: comparison with 1996/1997. *Atmos. Chem. Phys.*, *12*, 7073–7085. doi: 10.5194/acp-12-7073-2012

Kuttippurath, J., Kumar, P., Nair, P. J., & Pandey, P. C. (2018). Emergence of ozone recovery evidenced by reduction in the occurrence of Antarctic ozone loss saturation. *npj Clim. Atmos. Sci.*, *1*. doi: 10.1038/s41612-018-0052-6

Langematz, U., Meul, S., Grunow, K., Romanowsky, E., Oberländer, S., Abalichin, J., & Kubin, A. (2014). Future Arctic temperature and ozone: The role of stratospheric composition changes. *J. Geophys. Res. Atmos.*, *119*, 2092–2112. doi: 10.1002/2013JD021100

Lawrence, Z. D., Manney, G. L., & Wargan, K. (2018). Reanalysis intercomparisons of stratospheric polar processing diagnostics. *Atmos. Chem.Phys.*, *18*, 13547–13579. doi: 10.5194/acp-18-13547-2018

Livesey, N. J., Read, W. G., Wagner, P. A., Froidevaux, L., Lambert, A., Manney, G. L., ... Lay, R. R. (2020). *Earth Observing System (EOS) Aura Microwave Limb Sounder (MLS) version 4.2x level 2 and 3 data quality and description document.* JPL D-33509 Rev. E.

Livesey, N. J., Santee, M. L., & Manney, G. L. (2015). A Match-based approach to the estimation of polar stratospheric ozone loss using Aura Microwave Limb Sounder observations. *Atmos. Chem. Phys.*, *15*, 9945–9963. doi: 10.5194/acp-15-9945-2015

Manney, G. L., & Lawrence, Z. D. (2016). The major stratospheric final warming in 2016: dispersal of vortex air and termination of Arctic chemical ozone loss. *Atmos. Chem. Phys.*, *16*, 15371–153960.

Manney, G. L., Santee, M. L., Rex, M., Livesey, N. J., Pitts, M. C., Veefkind, P., ... Parrondo, M. C. (2011). Unprecedented Arctic ozone loss in 2011. *Nature*, *478*, 469-475.

Pommereau, J.-P., Goutail, F., Lefèvre, F., Pazmino, A., Adams, C., Dorokhov, V., ... van Roozendael, M. (2013). Why unprecedented ozone loss in the Arctic in 2011? Is it related to climate change? *Atmos. Chem. Phys.*, *13*, 5299–5308. doi: 10.5194/acp-13-5299-2013

Pommereau, J.-P., Goutail, F., Pazmino, A., Lefèvre, F., Chipperfield, M. P., Feng, W., ... Sitnikovah, V. (2018). Recent Arctic ozone depletion: Is there an impact of climate change? *Comptes Rendus Geoscience*, *350*(7), 347-353.

Remsberg, E., Natarajan, M., Marshall, B. T., Gordley, L. L., Thompson, R. E., & Lingenfelser, G. (2010). Improvements in the profiles and distributions of nitric acid and nitrogen dioxide with the LIMS version 6 dataset. *Atmos. Chem. Phys.*, *10*, 4741–4756. doi: 10.5194/acp-10-4741-2010

Rex, M., Salawitch, R., von der Gathen, P., Harris, N. R. P., Chipperfield, M., & Naujokat, B. (2004). Arctic ozone loss and climate change. *Geophys. Res. Lett.*, *31*(4). doi: 10.1029/2003GL018844

Rex, M., Salawitch, R. J., Deckelmann, H., von der Gathen, P., Harris, N. R. P., Chipperfield, M. P., ... Zerefos, C. (2006). Arctic winter 2005: Implications for stratospheric ozone loss and climate change. *Geophys. Res. Lett.*, *33*. doi: 10.1029/2006GL026731

Rex, M., von Der Gathen, P., Braathen, G., Harris, N., Reimer, E., Beck, A., ... Zerefos, C. (1999). Chemical ozone loss in the Arctic winter 1994/95 as determined by the Match technique. *J. Atmos. Chem.*, *32*, 35–59. doi: 10.1023/A:1006093826861

Rieder, H. E., & Polvani, L. M. (2013). Are recent Arctic ozone losses caused by increasing greenhouse gases? *Geophys. Res. Lett.*, *40*, 4437–4441. doi: 10.1002/grl.50835

Sinnhuber, B.-M., Stiller, G., Ruhnke, R., von Clarmann, T., Kellmann, S., & Aschmann, J. (2011). Arctic winter 2010/2011 at the brink of an ozone hole. *Geophys. Res. Lett.*, *38*(24). doi: 10.1029/2011GL049784

Smit, H. G. J., Straeter, W., Johnson, B. J., Oltmans, S. J., Davies, J., Tarasick, D. W., ... Posny, F. (2007). Assessment of the performance of ECC-ozonesondes under quasi-flight conditions in the environmental simulation chamber: insights from the Juelich ozonesonde intercomparison experiment (JOSIE). *J. Geophys. Res. Atmos.*, *112*. doi: 10.1029/2006JD007308

Solomon, S. (1999). Stratospheric ozone depletion: A review of concepts and history. *Rev. Geophys.*, *37*(3), 275-316.

Solomon, S., Garcia, R. R., Rowland, F. S., & Wuebbles, D. J. (1986). On the depletion of Antarctic ozone. *Nature*, *321*, 755-758.

Solomon, S., Haskins, J., Ivy, D. J., & Min, F. (2014). Fundamental differences between Arctic and Antarctic ozone depletion. *Proceedings of the National Academy of Sciences*, *111*(17), 6220–6225. doi: 10.1073/pnas.1319307111

Spang, R., Hoffmann, L., M´uller, R., Grooß, J.-U., Tritscher, I., H´opfner, M., ... Riese, M. (2018). A climatology of polar stratospheric cloud composition between 2002 and 2012 based on MIPAS/Envisat observations. *Atmos. Chem. Phys.*, *18*, 5089–5113. doi: 10.5194/acp-18-5089-2018

Strahan, S. E., Douglass, A. R., & Newman, P. A. (2013). The contributions of chemistry and transport to low Arctic ozone in March 2011 derived from Aura MLS observations. *J. Geophys. Res. Atmos.*, *118*(3), 1563-1576. doi: 10.1002/jgrd.50181

Tegtmeier, S., Rex, M., Wohltmann, I., & Krüger, K. (2008). Relative importance of dynamical and chemical contributions to Arctic wintertime ozone. *Geophys. Res. Lett.*, *35*. doi: 10.1029/2008GL034250

Tilmes, S., Müler, R., & Salawitch, R. (2008). The sensitivity of polar ozone depletion to proposed geoengineering schemes. *Science*, *320*(5880), 1201-1204.

Tilmes, S., Müller, R., Engel, A., Rex, M., & Russell III, J. M. (2006). Chemical ozone loss in the Arctic and Antarctic stratosphere between 1992 and 2005. *Geophys. Res. Lett.*, *33*(20). doi: 10.1029/2006GL026925

von der Gathen, P., Kivi, R., Salawitch, R. J., & Rex, M. (2020). The influence of climate change on chemical loss of ozone in the Arctic stratosphere. *submitted to Nature Climate Change*.

WMO. (2018). *World Meteorological Organization (WMO) / United Nations Environment Programme (UNEP), Scientific assessment of ozone depletion: 2018.* Global Ozone Research and Monitoring Project – Report No. 58.

Wohltmann, I., & Rex, M. (2009). The Lagrangian chemistry and transport model ATLAS: validation of advective transport and mixing. *Geosci. Model Dev.*, *2*, 153-173.